Theory of rapid-update line-by-line pulse shaping

John T. Willits,[1,2] Andrew M. Weiner,[1,3,*] and Steven T. Cundiff[1]

[1] *JILA, University of Colorado and National Institute of Standards and Technology, Boulder Colorado 80309-0440*
[2]*Department of Electrical and Computer Engineering, University of Colorado, Boulder, CO 80309-0425, USA*
[3] *Department of Electrical and Computer Engineering, Purdue University, West Lafayette, Indiana 47907-2035*
cundiffs@jila.colorado.edu

Abstract: Pulse shaping theory is extended to include rapid waveform update for line-by-line pulse shaping. The fundamental tradeoff between response speed and waveform fidelity is illustrated by several examples.

OCIS codes: (320.0320) Ultrafast optics; (320.5540) Pulse shaping

References and links

1. A. M. Weiner, "Femtosecond pulse shaping using spatial light modulators," Rev. Sci. Instrum. **71**, 1929-1960 (2000).
2. S. Xiao, A. M. Weiner, and C. Lin, "Experimental and theoretical study of hyperfine WDM demulitplexer performance using the Virtually Imaged Phased-Array (VIPA)," J. Lightwave Technol. **23**, 1456-1467 (2005).
3. S. A. Diddams, L. Hollberg, and V. Mbele, "Molecular fingerprinting with the resolved modes of a femtosecond laser frequency comb," Nature **445**, 627-630 (2007).
4. Z. Jiang, D.-S. Seo, D. E. Leaird, and A. M. Weiner, "Spectral line-by-line pulse shaping," Opt. Lett. **30**, 1557-1559 (2005).
5. Z. Jiang, C.-B. Huang, D. E. Leaird, and A. M. Weiner, "Optical arbitrary waveform processing of more than 100 spectral comb lines," Nat. Photonics **1**, 463-467 (2007).
6. D. J. Jones, S. A. Diddams, J. K. Ranka, A. Stentz, R. S. Windeler, J. L. Hall, and S. T. Cundiff, "Carrier-envelope phase control of femtosecond mode-locked lasers and direct optical frequency synthesis," Science **288,** 635-639 (2000).
7. J. Ye and S. T. Cundiff, eds., *Femtosecond Optical Frequency Combs Technology: Principle, Operation, and Application* (Springer, New York, 2004).
8. O. E. Martinez, "Grating and prism compressors in the case of finite beam size," J. Opt. Soc. Am. B **3**, 929-934 (1986).
9. R. N. Thurston, J. P. Heritage, A. M. Weiner, and W. J. Tomlinson, "Analysis of picoseconds pulse shape synthesis by spectral masking in a grating pulse compressor," IEEE J. Quantum Electron. **22**, 682-696 (1986).
10. M. M. Wefers and K. A. Nelson, "Space-time profiles of shaped ultrafast optical waveforms," IEEE J. Quantum Electron. **32**, 161-172 (1996).
11. J. Paye and A. Migus, "Space-time Wigner functions and their application to the analysis of a pulse shaper," J. Opt. Soc. Am. B **12**, 1480-1491 (1995).
12. R. D. Nelson, D. E. Leaird, and A. M. Weiner, "Programmable polarization-independent spectral phase compensation and pulse shaping," Opt. Express **11**, 1763-1769 (2003).
13. H. P. Sardesai, C-.C Chang, and A. M. Weiner, "A femtosecond code-division multiple-access communication system testbed," J. Lightwave Technol. **16**, 1953-1964 (1998).
14. Z. Bor and B. Racz, Opt. Commun. **54,** 165-170 (1985)
15. F.J. Harris, "Spectral analysis windowing," Wiley Encyclopedia of Electrical and Electronics Engineering, (Wiley, New York, 1999) Vol. 20, pp. 88-105.
16. J. W. Goodman, *Introduction to Fourier Optics* (McGraw-Hill, New York, 1968)
17. H. A. Haus, *Waves and Fields in Optoelectronics* (Prentice-Hall, Englewood Cliffs, New Jersey, 1984)

1. Introduction

The ability to manipulate the shape of broadband optical pulses has impacted many fields such as coherent control of chemical processes, high field physics, nonlinear fiber optics, and ultrafast spectroscopy [1]. Many methods have been invented to shape pulses, but the most widespread and general method for pulse shaping is spectral masking. In this method, the

#89804 - $15.00 USD Received 15 Nov 2007; revised 27 Dec 2007; accepted 28 Dec 2007; published 4 Jan 2008

spectral components of the laser pulses are spatially dispersed using an element such as a grating, and then a mask is applied to modify the phase and/or amplitude of each component. Finally, the components are recombined to reconstruct the new, modified pulses [1]. Using high resolution spectral dispersers such as a virtually imaged phased-array (VIPA) [2], the individual frequencies that comprise the spectral comb produced by a mode-locked laser can be resolved [3]. In this regime one can fully control the shape of a stream of pulses with line-by-line pulse shaping [4,5]. The limit that the update rate approaches the f_{rep} (repetition rate), where each pulse is individually shaped, is often referred to as arbitrary waveform generation. The ability to perform line-by-line pulse shaping on the output of a mode-locked laser has been enabled by the development of femtosecond comb techniques [6,7].

Current pulse shapers are good at producing waveforms of almost any shape at slow update rates. The output pulse shape for line-by-line pulse shaping is limited only by the spectral bandwidth. Most spatial light modulators used for this purpose operate at speeds less than 10 kHz, whereas mode-locked laser typically have an f_{rep} of 100MHz-1GHz. However, it is possible to modulate light at faster speeds with modulators such as $LiNbO_3$ or electro-absorption modulators. An array of fast modulators could be used in a pulse shaper and potentially shape each individual pulse. Here, we analyze the dynamics of the shaped pulses as the update rate approaches the repetition rate of the laser, f_{rep}. Our results illustrate that there is a fundamental tradeoff between response speed and waveform fidelity when high speed modulators are merged with line-by-line resolution. These trade-offs are fundamental and not due to limitations in modulator technology.

The naïve expectation of pulse shaping is that the instantaneous optical pulse will correspond to the instantaneous spectral mask; however this is not the case. Fast modulation creates sidebands that interfere with adjacent comb lines, causing degradation of spectral resolution. The Fourier time-frequency limit constrains how quickly the waveform can change given high spectral resolution. Lowering the spectral resolution degrades the fidelity of the generated waveform. Optimum performance between these fundamental limits is obtained when a tradeoff between these two extremes is made.

2. Theory

In this section, we derive a theoretical expression for Fourier transform pulse shaping with a time-varying mask. We begin by reviewing the theory for the familiar case of a time-independent mask, then show how to extend the theory to include time variation. Our treatment draws on previous publications analyzing grating pair compressors [8] as well as pulse shapers with static masks [9,10].

We start by writing the input field immediately before the first diffraction grating, as

$$e_{in}(x,t) = Re\left\{\hat{e}_{in}(x,t)e^{j\omega_o t}\right\} = Re\left\{a_{in}(t)s(x)e^{j\omega_o t}\right\} \tag{1}$$

Where x is spatial distance in one dimension, t is time, a_{in} is the input pulse train, and ω_0 is the angular frequency of the input. For simplicity later, we will use the notation $F(x,t) = Re\left\{\hat{F}(x,t)e^{j\omega_o t}\right\}$. We will take the input spatial profile as Gaussian, i.e.,

$$s(x) = e^{-x^2/w_{in}^2} \tag{2}$$

where w_{in} is the input spot size. We will assume a standard pulse shaping configuration, in which the grating and the pulse shaping mask are placed at the front and back focal planes of the lens, respectively. As shown in the Appendix, the field at the Fourier plane is

#89804 - $15.00 USD Received 15 Nov 2007; revised 27 Dec 2007; accepted 28 Dec 2007; published 4 Jan 2008

$$\hat{e}_1(x,t) \sim \int \frac{d\tilde{\omega}}{2\pi} A_{in}(\tilde{\omega}) e^{-\frac{(x-\alpha\tilde{\omega})^2}{w_0^2}} e^{j\tilde{\omega}t} \tag{3}$$

where $A_{in}(\tilde{\omega})$ is the Fourier transform of $a_{in}(t)$,

$$w_0 = \left(\frac{f\lambda}{\pi w_{in}}\right)\left(\frac{\cos\theta_i}{\cos\theta_D}\right) \tag{4}$$

is the radius of the focused beam at the Fourier plane (for any single frequency component), and

$$\alpha = \frac{\lambda^2 f}{2\pi c d \cos\theta_D} \tag{5}$$

is the spatial dispersion parameter that describes the proportionality between spatial displacement and optical frequency. The grating input and output (diffraction) angles are θ_i and θ_D respectively for a reference ray at frequency ω_0 traveling along the optical axis, d is the grating periodicity, and f is the focal length [1]. Now we add the spatial mask, with a complex transmission that we denote as $M(x)$, which is the key to pulse shaping action. The field directly after the mask is simply

$$\hat{e}_2(x,t) = M(x)\hat{e}_1(x,t). \tag{6}$$

Since for any specific frequency, the spot size is always finite at the masking plane, in general, the electric field subsequent to the spatial mask is a nonseparable function of space and frequency. This nonseparability occurs because the spatial profiles of the focused spectral components may be altered by the mask - i.e., some spectral components may sense spatially varying amplitude or phase, while others may not. This variation leads to different diffraction effects for different spectral components and results in an output field which couples space and time beyond the simple and reversible effects of spectral dispersion [10,11].

On the other hand, from an applications perspective, one is usually interested in generating a spatially uniform output beam with a single prescribed temporal profile. In order to obtain an output field that is a function of frequency (or time) only, one must perform an appropriate spatial filtering operation. In the following, we analyze the case where such spatial filtering is implemented by focusing into a single-mode optical fiber placed in a Fourier plane of the second diffraction grating [1,9]. This situation is of practical interest for applications related to optical communications. In a fiber-pigtailed reflection geometry pulse shaper, for example, the input beam is collimated from and the output beam is coupled back into the same physical fiber [12,13]. A similar mode selection operation could also be performed by coupling into a regenerative amplifier for high-power applications. Approximately, such spatial filtering can be performed simply by placing an iris after the pulse shaping setup.

For our analysis, we are interested in taking the masked field, propagating it to a second grating placed at the back focal plane of a second lens, and then focusing through a Fourier transform lens into a single mode fiber. The portion of the field that corresponds to the single guided spatial mode of the fiber is transmitted; any remaining portion of the field is not guided and is therefore eliminated. Denoting the spatial mode of the fiber as u_F and the field at the fiber plane as $\hat{e}_3$, the coupled field is

#89804 - $15.00 USD Received 15 Nov 2007; revised 27 Dec 2007; accepted 28 Dec 2007; published 4 Jan 2008

$$\hat{e}_{out}(x,t) = \frac{\int dx\, \hat{e}_3(x,t) u_F^*(x)}{\int dx\, u_F(x) u_F^*(x)}\, u_F(x)\,. \tag{7}$$

Here the first factor gives the complex amplitude of the coupled field, and the second is the spatial mode. The most interesting case is when the input field as transformed by the pulse shaper and the subsequent lens is perfectly mode-matched to the fiber. In the absence of masking, the entire input field is successfully coupled into the fiber without loss. In this case the output complex spectral amplitude function becomes

$$A_{out}(\tilde{\omega}) = \left\{ \sqrt{\frac{2}{\pi w_o^2}} \int dx\, M(x) \left[\exp\left(\frac{-(x-\alpha\tilde{\omega})^2}{w_o^2} \right) \right]^2 \right\} A_{in}(\tilde{\omega})\,. \tag{8}$$

The effective filter in the frequency domain is the square of the convolution of the mask function $M(x)$ and the spatial field profile of the beam at the masking plane. Note that the spatial field profile enters once through the spectral dispersion of the first grating and lens and a second time (together with an integral over x) through the mode matching with an assumed Gaussian fiber mode. Any physical features on the mask smaller than $\sim w_o$ are smeared out by the convolution, and this limits the finest features which can be transferred onto the spectrum. Wavelength components impinging on mask features that vary too fast for the available spectral resolution are in part diffracted out of the main beam and eliminated by the spatial filter. This process can lead to phase-to-amplitude conversion in the pulse shaping process [8,12]. Conversely, in the limit $w_o \to 0$, the apparatus provides perfect spectral resolution, and the effective filter is just a scaled version of the mask.

We may now extend the theory to include a time-varying mask, $M(x,t)$, with Fourier transform

$$\tilde{M}(x,\omega) = \int dt\, M(x,t) e^{-j\omega t}\,. \tag{9}$$

The complex spectral amplitude of the field immediately after the masking operation is

$$A_2(x,\tilde{\omega}) \sim \int \frac{d\tilde{\omega}'}{2\pi} A_{in}(\tilde{\omega}-\tilde{\omega}') M(x,\tilde{\omega}') e^{-\frac{\left(x-\alpha(\tilde{\omega}-\tilde{\omega}')\right)^2}{w_o^2}}\,. \tag{10}$$

The time-varying mask modifies the frequency content at the various spatial locations. Mode matching at the output of the pulse shaper is taken into account giving

$$A_{out}(\tilde{\omega}) \sim \iint \frac{d\tilde{\omega}'}{2\pi} dx\, A_{in}(\tilde{\omega}-\tilde{\omega}') M(x,\tilde{\omega}') e^{-\frac{\left(x-\alpha(\tilde{\omega}-\tilde{\omega}')\right)^2}{w_o^2}} e^{-\frac{(x-\alpha\tilde{\omega})^2}{w_o^2}}\,. \tag{11}$$

The interpretation is that for large frequency shifts, the new frequencies induced through the time variation of the mask will be focused at a position transversely shifted with respect to the fiber mode. As a result, the higher modulation frequencies of the time-varying mask are partially suppressed.

A very simple case is when the mask is time-varying but uniform in space; the time-varying mask is simply a modulator placed into a pulse shaper. Replacing $M(x,\tilde{\omega})$ in Eq. (11) with $M(\tilde{\omega})$ yields

#89804 - $15.00 USD Received 15 Nov 2007; revised 27 Dec 2007; accepted 28 Dec 2007; published 4 Jan 2008

$$A_{out}(\tilde{\omega}) \sim \int \frac{d\tilde{\omega}'}{2\pi}\left(M(\tilde{\omega}')e^{-\alpha^2(\tilde{\omega}')^2/2w_o^2}\right)A_{in}(\tilde{\omega}-\tilde{\omega}') \quad (12)$$

Here the modulation spectrum is multiplied by a low-pass filter function. As the spot size at the masking plane gets smaller, the low pass filter cuts off at lower frequencies, revealing a fundamental trade-off in pulse shaping: very high spectral resolution implies a limit to the rate at which the pulse shaping function may be modified. In line-by-line shaping, the implication is that one may not fully update pulse shapes at speeds corresponding to the laser repetition rate while simultaneously fully resolving individual comb lines.

3. Simulation

The dynamic effects of a pulse shaper can be illuminated by numerical simulation. The simulation numerically calculates the double integral in Eq. (11). The input and output spectra are represented by arrays that contain the input and output frequency comb of the pulse train, while the spectral mask is a matrix that fully describes the mask in space and time. In the integral, the mask is represented as a space and ω' dependent matrix, which is equivalent to taking the one-dimensional Fourier transform of the temporal response of the mask at each spatial point. An array size of 256 pixels was chosen to balance resolution and computation time. The input spectrum is an array of 0's with a spike of 1 every 8 pixels enveloped in a Gaussian. By taking the Fourier Transform of this array we can construct the input train of pulses as a function of time (Fig. 1).

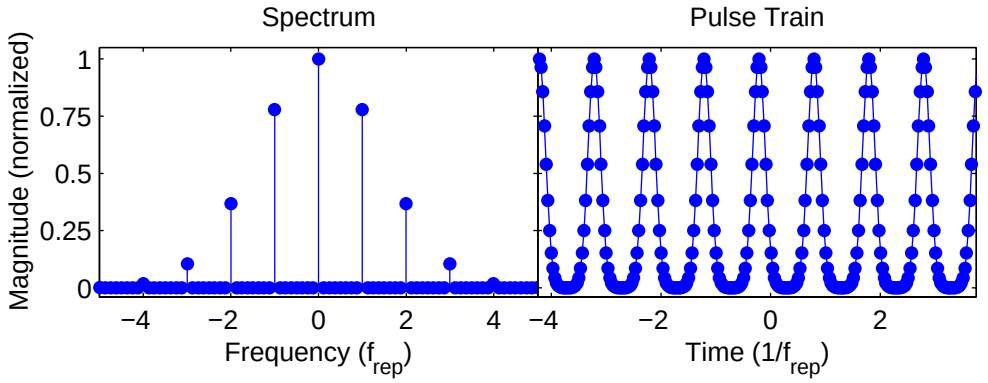

Fig. 1. Input spectrum and pulse train.

The relationship between α and w_0 sets the width of the Gaussian "smearing" functions in Eq. (11) that determine the response of the pulse shaper. The narrower the Gaussians, the slower the response to changes in the mask. Conversely, the broader the Gaussians are, the more blurred or poorly resolved the spectral response of the mask. Poor resolution results in low waveform fidelity and excessive resolution results in slow response speeds. The result is a fundamental trade-off between spectral resolution and response time.

To investigate the effects of the smearing functions on pulse shaping, w_0 is varied, which changes the width of the smearing functions. Both α and w_0 are set by the specific design of a given pulse shaper with a dependence on parameters like wavelength and focal length of the lens used in the pulse shaper as described by Eq. (4) and Eq. (5). Since we are looking at a narrow band of frequencies the effect of wavelength on this ratio is not important to the illustrated fundamental trade-off. The variation of w_0 is equivalent to setting the spacing between the comb lines on a spectral mask then adjusting the focus of the comb lines to change their size. For generality w_0 is expressed as a fraction of

#89804 - $15.00 USD Received 15 Nov 2007; revised 27 Dec 2007; accepted 28 Dec 2007; published 4 Jan 2008

$$w_{rep} = 2\pi\alpha f_{rep}. \quad (13)$$

For example, for a 1 GHz laser with the individual comb lines by dispersed by 20 μm, w_{rep} is 20 μm and α is 20 μm/2πGHz. So $w_0 = ½\ w_{rep} = \pi f_{rep}\alpha$ is 1/2 the distance between comb lines or 10 μm.

4. Results

In a first set of test cases, dynamic effects are seen in the response of the pulse train to a step. A sample of pulses is analyzed by abruptly changing the spectral mask at time 0. Before time 0, the spectral mask allows the full spectrum to pass, and after time 0, it blocks every other comb line as illustrated in Fig. 2.

The mask pattern for $t > 0$ doubles the separation between comb lines in frequency space, which makes the time between pulses half as long, or in effect doubles f_{rep}. Figure 3 shows the switching behavior of the pulse train at various smearing function widths or spot sizes, w_0. Due to the periodic nature of the Fast Fourier Transform algorithm, transient effects were observed at both edges of time aperture used in the simulation. These expected edge effects are cropped out of the final pulse trains in order to simplify the appearance of Fig. 3. This simplification was done by doubling the sample size of the input and then cropping the final output by deleting the first and last quarter leaving the same number of pulses. For large spot sizes such as $w_0 = w_{rep}$, the spectral blurring due to a broad smearing function is quite evident. In the spectral domain, this effect is seen in Fig. 2, which plots the effective static filter functions corresponding to the mask at time $t > 0$. The edges of the filter function become increasingly rounded for increasing w_0 due to the convolution of the mask with the smearing function. In the time domain, as the spot size increases and the smearing function becomes broader, the ability of the shaper to produce clear double pulses is diminished. In Fig. 3, observe the red dotted line for the larger spot sizes and how it peaks at two different heights; this poor waveform is due to the overlapping of the power associated with different comb lines at the same position on the mask. At smaller spot sizes the spectral resolution is improved, with the result that the pulses in the doubled repetition rate region ($t > 0$) have equal intensities. However, the dynamic response suffers. The $w_0 = 1/8\ w_{rep}$ case shows how slowly the pulse train responds to change when the smearing function is narrow; the system takes about 4 repetition periods to shift to double pulsing while at $w_0 = w_{rep}$ it shifts almost instantly. The key point is that response to an abrupt change in the mask occurs over a time duration that scales inversely with the spectral resolution. Qualititatively speaking, the optimum spot size for the system described above that balances speed and spectral resolution (waveform fidelity) is approximately $w_0 = 3/8\ w_{rep.}$ This means that the spot size of the comb lines on the spectral mask should be approximately 1/3 the distance between comb lines, although the exact choice will depend on the specific merit function of interest.

#89804 - $15.00 USD Received 15 Nov 2007; revised 27 Dec 2007; accepted 28 Dec 2007; published 4 Jan 2008

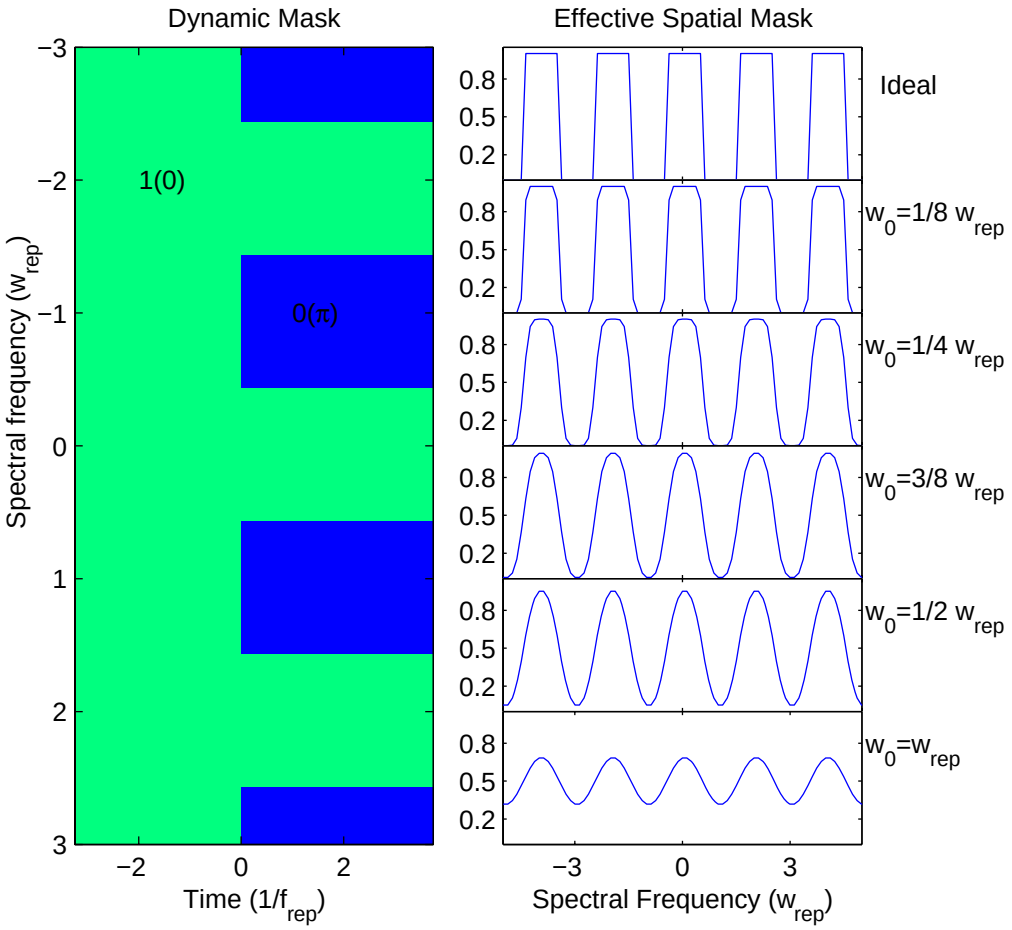

Fig. 2. Dynamic masks and effective spectral filter functions. Left: the dynamic mask illustrates the abrupt change in the mask at time 0. Two cases are considered. For spectral amplitude masking, the mask is set to block every other comb line for $t > 0$; the blue regions in the figure correspond to a mask value of 0. For spectral phase masking, the mask is set to impart a phase shift of π to every second comb line as illustrated by the blue regions in the figure. Right: the static filter functions corresponding to times $t > 0$ illustrate the blurring of the effective mask for larger spot sizes. The effective spatial masks are calculated by convolving the smearing function in Eq. (11) with the spatial mask.

We note that the pulse train output appears to be affected prior to the step in the mask at $t = 0$. However, due to the large delay in propagating through the pulse shaper (not portrayed in the figures), there is no violation of causality. Apparent changes in the output waveform prior to $t = 0$ simply correspond to the components of light being deflected or diffracted to shorter paths through the shaper. Consistent with this interpretation, the analysis in [10] for a static pulse shaper shows a direct linkage between delay time in the shaped output waveform and spatial offset in the output beam (here without spatial filtering). We also observe that angular dispersion from a grating or other spectral disperser is linked fundamentally to delay gradients across the beam [14]. Waveform changes in response to a step in the mask occur within a time region approximately equal to the inverse of the spectral resolution, which is consequently within the total time variation across the beam just after the spectral disperser.

#89804 - $15.00 USD Received 15 Nov 2007; revised 27 Dec 2007; accepted 28 Dec 2007; published 4 Jan 2008

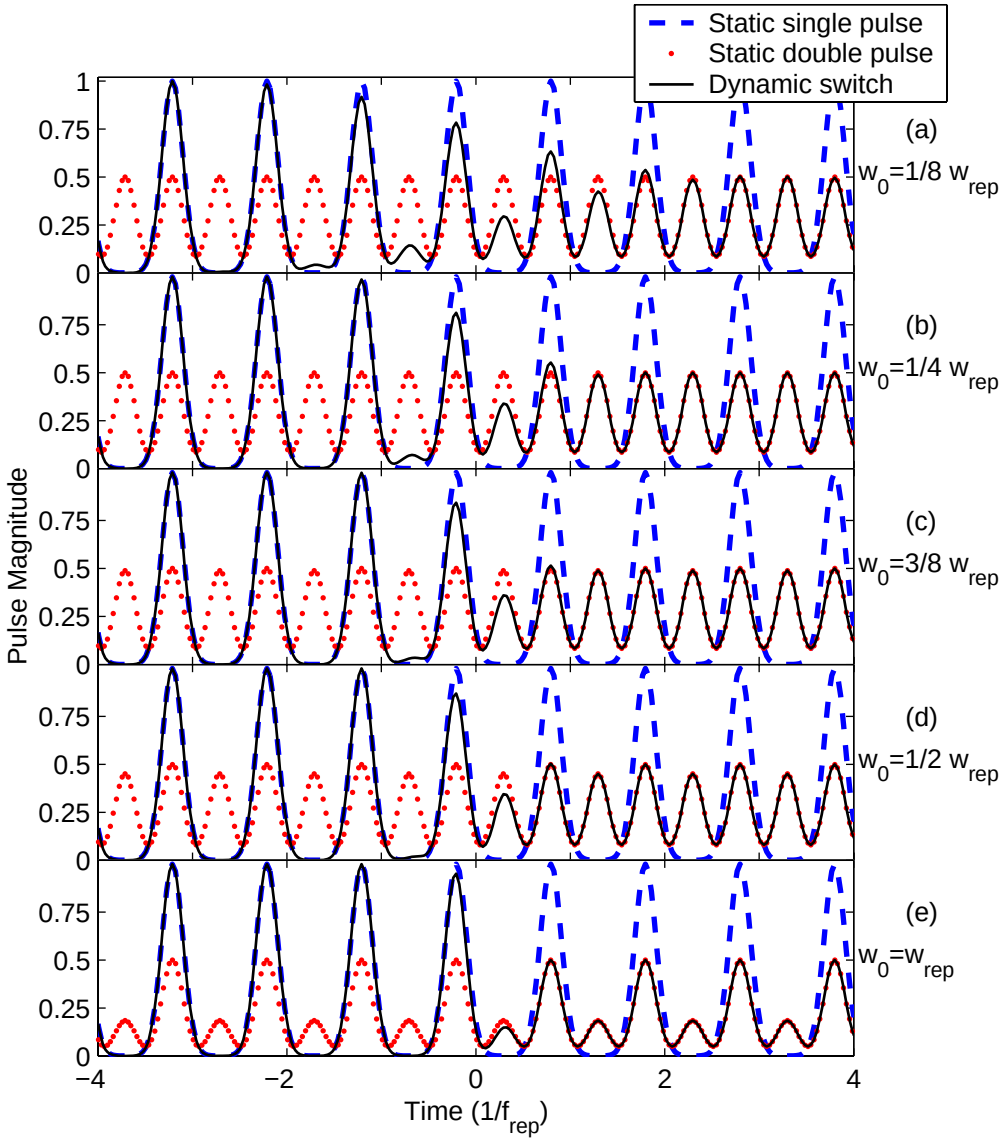

Fig. 3. Response of the pulse train to an alternating amplitude mask, turned on abruptly at $t = 0$, for various spot sizes, w_0. The dashed blue line shows the static pulse train where the full spectrum is allowed to pass, which yields the expected single pulsing. The dotted red line shows the static pulse train when every other comb line in the spectrum is masked out. This results in double pulsing behavior, with waveform fidelity that depends on w_0. The solid black line shows the dynamic response of a pulse train to the mask that abruptly switches at $t = 0$.

In a second example, we consider a stepped phase mask. A phase shift of π between alternating comb lines is turned on abruptly at $t = 0$. Both the physical phase mask and the static spectral filter function (corresponding to $t > 0$) are also shown in Fig. 2. The filter function is the same as for the amplitude mask case, but the vertical axis corresponds to the phase of the mask alternating between 0 and π (complex transmission alternates between (1,0) and (-1,0)). The output pulse train can be seen in Fig. 4. For high resolution static pulse shaping, the mask is expected simply to shift the output in time by half the period of the pulse train. Similar to what was seen in the amplitude case, we have fast response for large w_0 but with waveform fidelity compromised (this is evident in this case as a reduction in

#89804 - $15.00 USD Received 15 Nov 2007; revised 27 Dec 2007; accepted 28 Dec 2007; published 4 Jan 2008

intensity). Conversely for small w_0 we have high spectral resolution and good waveform fidelity (negligible loss of intensity) but slow response. Again the optimum spot size appears to be approximately 1/3 the distance between comb lines.

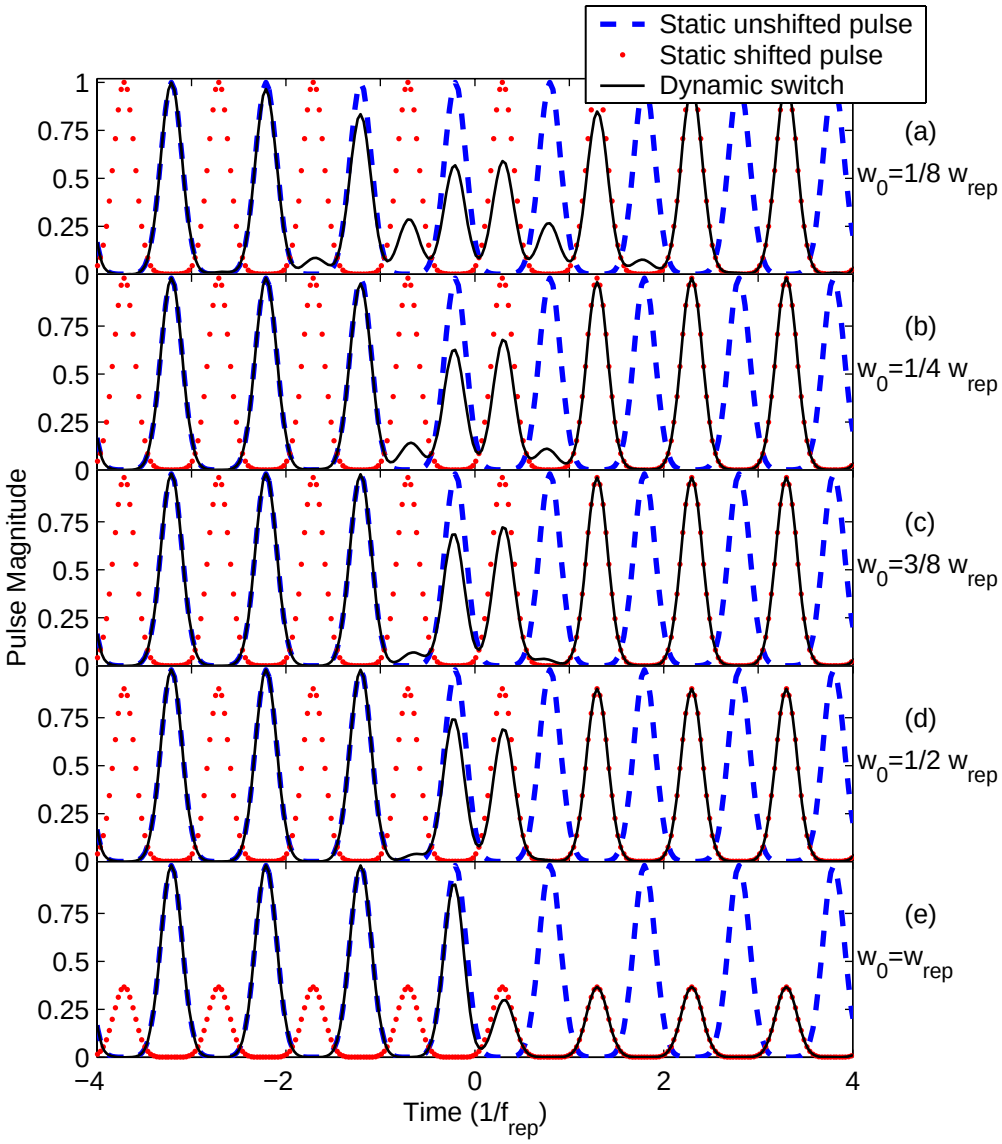

Fig. 4. Response of the pulse train to an alternating phase mask, turned on abruptly at t=0, at various spot sizes, w_0. The dashed blue line shows the static pulse train where the full spectrum is allowed to pass with no phase shift. The dotted red line shows the static pulse train when every other comb line in the spectrum is phase shifted by π; this yields the expected shift of half the period in the output pulse train. The solid black line shows the dynamic response of a pulse train to a mask that abruptly switches between the two at $t = 0$.

Another test case that illustrates the dynamic behavior of the pulse shaper is its response to a sweeping bandpass spectral filter. Here the mask blocks the full spectrum except for a square window. This pass window is then shifted spatially as a function of time allowing different portions of the spectrum to pass at different times. The window scans through the center of the spectrum at a rate of $2/9\ w_{rep}f_{rep}$. For this case, a larger α was used to give greater separation of the comb lines. Thus, instead of having a comb line every 8 pixels now

#89804 - $15.00 USD Received 15 Nov 2007; revised 27 Dec 2007; accepted 28 Dec 2007; published 4 Jan 2008

there is a comb line every 24 pixels. Also for this calculation, all the input comb lines were set to unity amplitude, so the spectral envelope is flat rather than Gaussian. The width of the window was set to 24 pixels corresponding to w_{rep} in space or f_{rep} in frequency, such that ideally, one comb line is allowed through the mask at a time. The response of the pulse train to this sweeping filter can be seen in Fig. 5. At the top of this figure is the ideal case, a pseudo-spectrogram that shows how one might naïvely expect the system to respond to the moving filter, allowing one comb line through at a time. This pseudo-spectrogram is created simply by multiplying the input spectrum by a scaled version of the time-dependent mask (no smearing taken into account), and then the comb line is broadened appropriately by the inverse time window chosen to construct the figure.

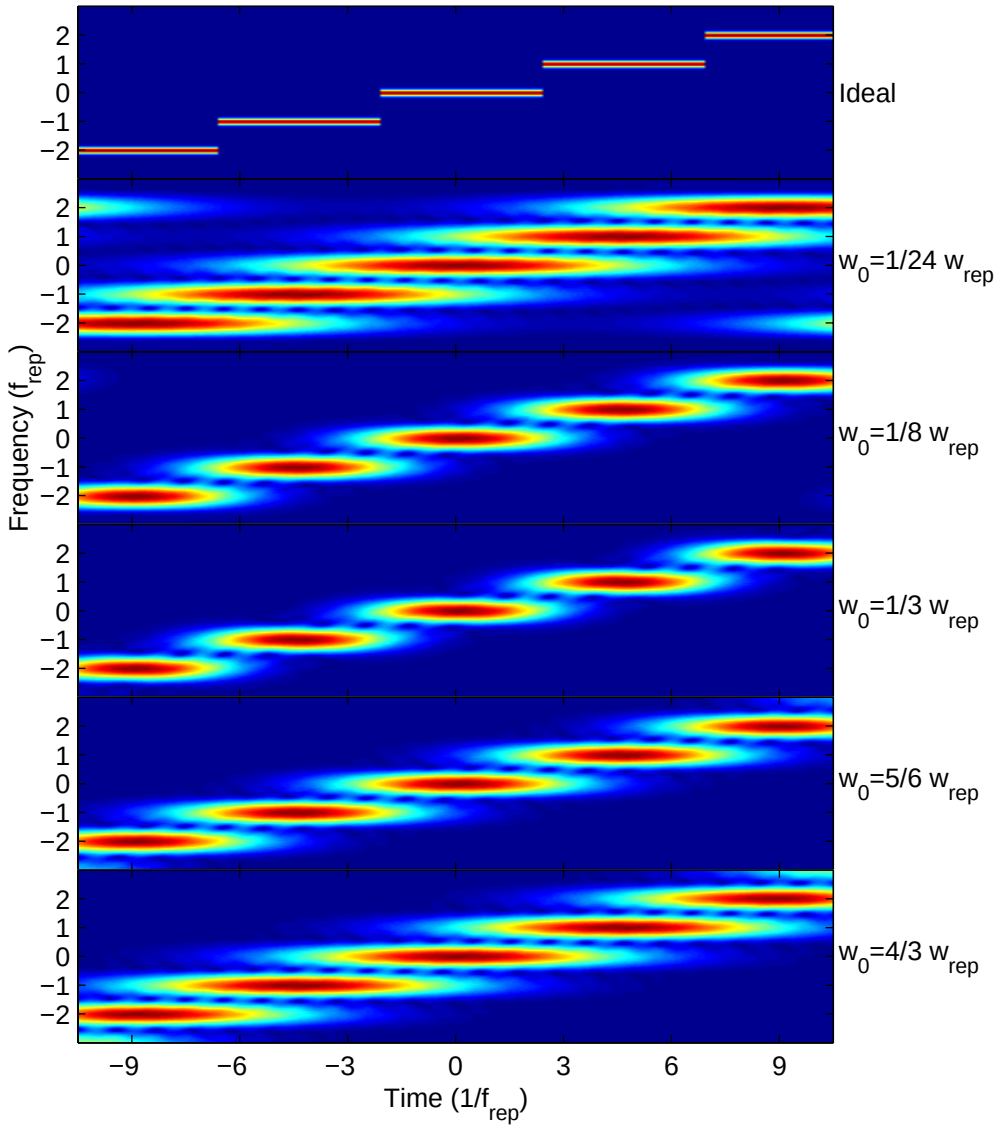

Fig. 5. Spectrogram response of a pulse train with equal size comb lines to a sliding spectral window of size f_{rep} for various spot sizes, w_0. The ideal case is a pseudo-spectrogram of what one would naively expect from a moving spectral filter.

#89804 - $15.00 USD Received 15 Nov 2007; revised 27 Dec 2007; accepted 28 Dec 2007; published 4 Jan 2008

The spectrograms for the actual simulated output signals at various spot sizes were created using a gate function set equal to the Hanning window [15] with a size of 32 pixels; this means that the spectrogram at each point in time is the result of the frequency response of the sample inside this window 16 pixels before and 16 pixels after the point in time being calculated. The behavior of these spectrograms may be explained in terms of the smearing function, as previously discussed. When the spot size is small, the static filtering function that would be obtained for a stationary bandpass mask is sharp, as seen in Fig. 6. On the other hand, the narrow smearing function slows the response of the pulse train to changes in the mask. This slowing of the response is evident in the w_0=1/24 w_{rep} spectrogram where the traces are elongated along the time axis. As w_0 increases, the spectrograms initially shrink along the time axis, attaining a minimum extent around w_0=1/3 $w_{rep,}$ but then elongate once again. This minimum in duration is explained on the basis of the blurring of the equivalent static filtering functions depicted in Fig. 6. For large w_0 the equivalent static filters are unable to resolve individual lines, and the filter must be tuned over a larger frequency range (which requires more time) before a given comb line is cut off. Thus the seemingly slow response at w_0=4/3 w_{rep} arises from the the rounded edges of the effective mask; since we are analyzing the response of the system to a moving filter, the spectral blurring affects how the system appears to respond in time.

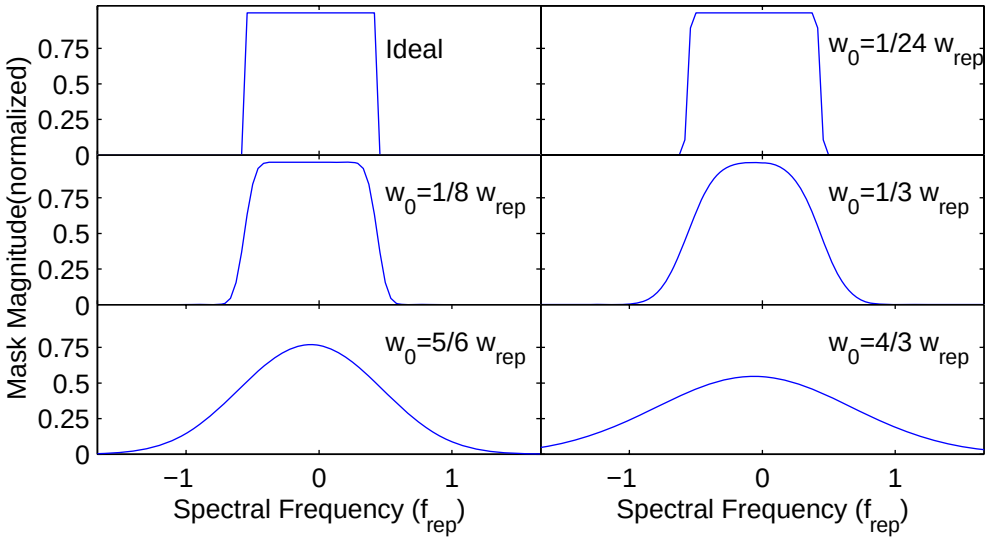

Fig. 6. Sliding filter effective masks at various w_0 as it the window crosses the center of the spectrum.

The magnitude of the output waveform can be seen in Fig. 7 for three spot sizes. The ideal case where only a single frequency is selected at a time would result in a constant, time-independent field amplitude. This behavior is most closely approximated by the w_0=1/3 w_{rep} case. However, in all cases where multiple frequencies are present there is modulation in the time domain field magnitude. This effect is minimized for intermediate values of spot size such as w_0=1/3 w_{rep}. When the spot size is either substantially decreased or increased, more frequencies are simultaneously present, and much stronger structure is observed in the time domain waveforms.

5. Summary

The dynamic effects of fast pulse shaping have been analyzed and explored in three representative cases. In all these test cases, the spot size of the comb lines on the spectral mask is varied to adjust the width of the smearing function and thereby observe the effects on

#89804 - $15.00 USD Received 15 Nov 2007; revised 27 Dec 2007; accepted 28 Dec 2007; published 4 Jan 2008

the output pulse train. The first case is a step in amplitude of alternating comb lines. By removing every other comb line, the shaper produces a double pulsing output. The pulse train responds quickly with poor spectral resolution when the smearing function is broad. The second case also illustrates this effect by an abrupt phase shift in alternating comb lines by π, which shifts the output pulse train by half the period. Again, we see similar dynamic effects. The final case describes the response of the pulse train to a sliding spectral filter. Interestingly we see similar effects for broad and narrow smearing functions; this is explained through the dynamic spatial nature of the mask. All these test cases demonstrate that there is an optimum spot size or width of the smearing function that balances speed and spectral resolution. This optimum is achieved when the radius of the spot size of the comb lines on the spectral mask is approximately one third the distance between comb lines.

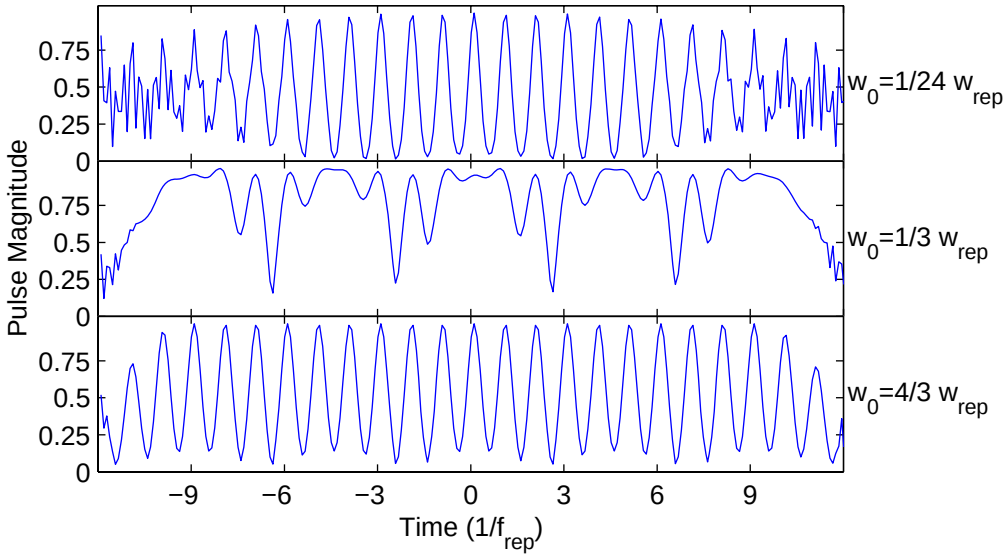

Fig. 7. Electric field magnitude for a pulse train passed through a pulse shaper with a sliding spectral window of size f_{rep} for various spot sizes, w_0. Since the tunable filter ideally allows only one comb through at a time, the ideal pulse train would be converted to a constant magnitude, with no oscillation. We see that w_0=1/3 w_{rep} is the closest we get to this ideal response with minimal oscillations in the region where the tunable filter shifts between comb lines.

It is worth emphasizing that our analysis applies specifically to the case where the output Gaussian mode filter is precisely matched to the field that propagates through the pulse shaper in the absence of masking. Usually this will be the most interesting case, as it minimizes loss. However, new effects may be possible for other choices of the output mode filter. For example, if the mode filter is spatially offset from the optimum position, it will lead to bandpass rather than low-pass filtering action of a rapidly varying pulse shaping mask. In this case a simple time-varying amplitude or phase mask could be used, for example, to impose single-sideband modulation in parallel onto an entire set of optical comb lines.

Acknowledgments

Funding for this project was provided by NIST. AMW also acknowledges funding from the National Science Foundation under Grant ECCS-0601692.
*Purdue is Andrew Weiner's current and permanent location

#89804 - $15.00 USD Received 15 Nov 2007; revised 27 Dec 2007; accepted 28 Dec 2007; published 4 Jan 2008

Appendix A. Field at the masking plane

Assuming an input field prior to the grating as given by Eq. (1), the field immediately after the grating may be written as [8]

$$e'_{in}(x,t) = \sqrt{\beta_a}\, Re\left\{\int \frac{d\tilde{\omega}}{2\pi} A(\tilde{\omega}) s(\beta_a x) e^{-j\gamma\tilde{\omega}x} e^{j(\omega_o+\tilde{\omega})t}\right\} \tag{A.1}$$

where $\beta_a = \frac{\cos\theta_i^{(o)}}{\cos\theta_D^{(o)}}$ and $\gamma = \frac{2\pi}{\omega_o d \cos\theta_D^{(o)}}$. Here $\cos\theta_i^{(o)}$ and $\cos\theta_D^{(o)}$ are the input and output (diffraction) angles for a reference ray at frequency ω_o traveling along the optical axis, and d is the grating periodicity. The $e^{-j\gamma\tilde{\omega}x}$ factor imparts the variation in diffraction angle with frequency; and the beam size is scaled by the inverse of an astigmatism factor β_a, which results from the difference in input and output angles.

Propagation from the grating at the front focal plane of the lens to the masking plane at the back focal plane may be analyzed using the Fourier transform property of a lens [16,17]. Specifically, for a scalar, monochromatic, one-dimensional field $s_{in}(x)$ at a plane a distance f in front of a thin lens with focal length *f*, the resulting field at an output plane a distance *f* behind the lens is

$$s_{out}(x) = \sqrt{\tfrac{j}{\lambda f}} \int dx' s_{in}(x') e^{jkxx'/f} \sim S_{in}\left(\tfrac{kx}{f}\right) \tag{A.2}$$

where $k = \omega/c = 2\pi/\lambda$, and $S_{in}(k_x)$ refers to the spatial Fourier transform of the input spatial profile $s_{in}(x)$, and the Fourier transforms are defined as $S(k) = \int dx\, s(x) e^{jkx}$ and $s(x) = \frac{1}{2\pi}\int dk\, S(K) e^{-jkx}$. Using this Fourier transform property in conjunction with Eq. (A.1) for the field just after the grating, we immediately obtain the field at the masking plane of the pulse shaper, Eq. (3).

#89804 - $15.00 USD Received 15 Nov 2007; revised 27 Dec 2007; accepted 28 Dec 2007; published 4 Jan 2008